Atomic Spectroscopy

Article

Further Characterization of Four Natural Ilmenite Reference Materials for *in situ* Fe Isotopic Analysis

Hong Liu,[a] Yantong Feng,[a, b] Ming Li,[a] Zhaochu Hu,[a, *] Wen Zhang,[a] Zaicong Wang,[a] Tao Luo,[a] Liyuan Qing,[a] and Shenghong Hu[c]

[a] State Key Laboratory of Geological Processes and Mineral Resources, China University of Geosciences, Wuhan 430074, P. R. China

[b] Gansu Key Laboratory of Mineral Resources in Western China, School of Earth Sciences, Lanzhou University, Lanzhou 730000, P. R. China

[c] State Key Laboratory of Biogeology and Environmental Geology, China University of Geosciences, Wuhan 430074, P. R. China

Received: *November 19, 2023;* ***Revised:*** *December 30, 2023;* ***Accepted:*** *December 30, 2023;* ***Available online:*** *December 30, 2023.*

DOI: 10.46770/AS.2023.281

ABSTRACT: Iron (Fe) isotopic composition is a useful geochemical tracer. Because of the high spatial resolution and simple sample preparation, laser ablation multi-collector inductively coupled plasma mass spectrometry (LA-MC-ICP-MS) is becoming increasingly popular for Fe isotopic analysis. However, the matrix effect is a challenge for the LA-MC-ICP-MS technique, and external standardization using a matrix-matched reference material is essential. Ilmenite is a common and significant Fe-rich mineral phase in terrestrial and lunar rock, which has variable Cr contents. Herein, four natural ilmenites (RUS10, CZE2, SIN1, and GER16) with Cr contents of 15-2420 μg g^{-1} were characterized for Fe isotopic compositions by both solution nebulization (SN) MC-ICP-MS and LA-MC-ICP-MS. The protocol of isobaric interference correction (^{54}Cr on ^{54}Fe) was optimized for *in situ* Fe isotopic analysis. The precision and accuracy of ns-LA-MC-ICP-MS measurements are comparable to those of fs-LA-MC-ICP-MS for Fe isotopic analysis. The individual spot internal precision (2SE) of δ^{56}Fe was consistently better than 0.08‰ at ^{56}Fe signal intensity ≥10 V, and the analytical external precisions (2sd) of δ^{56}Fe were in a range from ±0.10‰ to ±0.16‰ in multiple ilmenite fragments by both ns-LA-MC-ICP-MS and fs-LA-MC-ICP-MS. The $\delta^{56}Fe_{IRMM-014}$ values of four ilmenites (RUS10, CZE2, SIN1, and GER16) were 0.22 ± 0.14‰ (2sd, n=165), 0.14 ± 0.14‰ (n=123), 0.00 ± 0.14‰ (n=110) and 0.00 ± 0.14‰ (n=164), respectively. The four ilmenites, found to be homogeneous in Fe isotopic compositions, are proposed as candidate reference materials to be shared with peers. These ilmenites with different Cr contents and positive Fe isotopic values would certainly be helpful as reference materials for the scientific community.

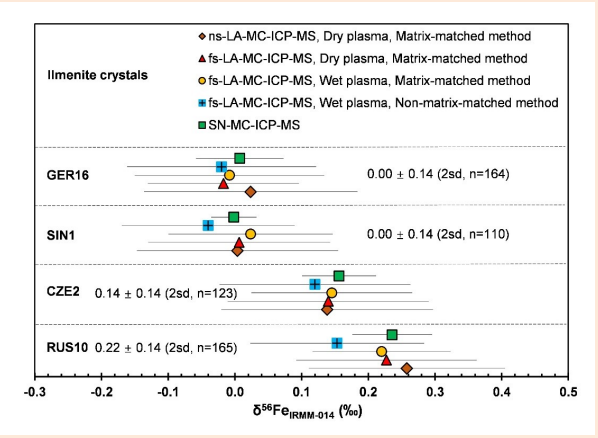

INTRODUCTION

Iron (Fe) isotopes are used to explore geochemical processes, including magma differentiation,[1-5] ore-deposit formation,[6,7] planetary evolution,[8-11] and weathering.[12,13] Significant Fe isotopic fractionation will occur in several common rock-forming minerals.[14, 15] In the last two decades, multi-collector inductively coupled plasma mass spectrometry (MC-ICP-MS) has become a powerful and routine technique for solution nebulization (SN) Fe isotopic analysis in geological materials.[16-19] Compared with SN-MC-ICP-MS, LA-MC-ICP-MS has the advantages of high spatial resolution, fast analysis and simple sample preparation.[20] It has been successfully applied to the measurements of Fe isotope ratios in pure Fe metal,[7,21,22] pyrite,[6,23,24] Fe-meteorites,[7] taenite,[7] hematite,[7, 25] siderite,[7] magnetite,[7] pyrrhotite,[24,26,27] glassy cosmic spherules,[28] chalcopyrite,[23, 25] USGS reference glasses,[29,30] and ilmenite.[22,31] The Fe isotopic compositions obtained from small-scale materials with complex structures offer some new views in geological processes, *e.g.*, magma differentiation[7] and hydrothermal processes.[32]

In situ Fe isotopic analysis is routinely conducted by LA-MC-ICP-MS using either a sample-standard-bracketing (SSB)

protocol[7,24,28,30] or a Ni element-doping (ED) and SSB combination protocol[22,31] to correct instrumental isotopic fractionation/mass bias. Here, the mass biases of the bracketing standard and the measured sample are assumed to be perfectly consistent during the whole measurement processes of laser ablation, aerosol transportation and mass spectrometric determination.[24] The differences between the bracketing standard and the unknown sample in physical property and chemical composition would result in biased isotope ratios for LA-MC-ICP-MS analysis.[24, 25, 31] It is necessary to minimize the matrix effect by characterizing matrix-matched reference materials[23,26,31,33] and/or developing non-matrix-matched calibration protocols[7,22,24,25,34] for *in situ* Fe isotopic analysis in different geological minerals by LA-MC-ICP-MS.

The femtosecond (fs) laser produces smaller sample particles than the nanosecond (ns) laser, which decreases the matrix effect by improving the efficiencies of aerosol transmission and ionization.[7,24] However, the matrix effect is still significant even with fs-LA-MC-ICP-MS under routine dry plasma conditions, *e.g.*, between magnetite and pyrite[24] and between Fe metal and pyrite.[31] The novel wet plasma conditions by introducing water into LA-MC-ICP-MS are helpful to minimize the matrix effect due to improved plasma conditions.[22-24,31] For instance, accurate results for pyrite and ilmenite were obtained by fs-LA-MC-ICP-MS under wet plasma conditions using Fe metal IRMM-524A as a bracketing standard.[22] Furthermore, the matrix effects among pyrite, hematite, chalcopyrite and magnetite are minimized by ns-LA-MC-ICP-MS with a robust combination of wet plasma and N_2 gas.[25] However, the introduction of water vapor and/or N_2 gas complicates the sampling system of LA-MC-ICP-MS analysis. In addition, these non-matrix-matched calibration protocols still need at least one matrix-matched reference material as a quality control standard (*i.e.*, secondary standard) to demonstrate analytical reliability and optimize instrumental parameters for *in situ* isotopic analysis. Effectiveness of non-matrix-matched methods is related to the daily state of the instrument, operating conditions, and experience of the operator, which may not be consistent among different laboratories.

Suitable reference materials are crucial for *in situ* Fe isotopic analysis. The certified Fe metal reference materials (IRMM-014 and IRMM-524A) can serve as excellent external reference materials by fs-LA-MC-ICP-MS.[7,22] Some Fe-rich minerals have been characterized for Fe isotopic homogeneity by LA-MC-ICP-MS, such as pyrite Aa018[25] and Tianyu-Py,[33] pyrrhotite Jc-Po and pentlandite Jc-Pn,[26] and ilmenite PZH12-24.[31] Natural reference material is rare and precious, because the Fe isotope shows a complex variation in geological process.[14] The pressed tablet of ultrafine natural mineral powder has become an alternative reference material, such as pyrite PAS-Py600 and chalcopyrite PAS-Cpy600.[23] The homogeneity of the natural mineral is improved by obtaining its ultrafine powder. Note that the physical properties of the pressed powder pellet (*e.g.*, hardness and density) are different from those of natural minerals. Therefore, the wet plasma protocol is still needed to minimize the potential matrix effect.[23]

Ilmenite ($FeTiO_3$) is a common Fe-rich mineral in magmatic rocks, sedimentary rocks, metamorphic rocks and lunar soils[4,35-41] and is used to obtain geochemical information, including U–Pb dating,[36] Hf isotopes,[42] Ti isotopes,[43,44] Fe isotopes,[22,31,45] and trace elements.[41,46] Ilmenite as a significant geological tool is used to explore lunar basalt petrogenesis and understand igneous geological processes.[1,15,36,38,39] Three ilmenites (*i.e.*, PZH12-16, PZH12-18 and PZH12-24) are reported as potential reference materials for *in situ* Fe isotopic analysis.[22,31] These ilmenite references with low Cr contents all have $\delta^{56}Fe_{IRMM\text{-}014}$ negative values relative to the IRMM-014 standard. The potential spectral interference of ^{54}Cr on ^{54}Fe is a challenge for LA-MC-ICP-MS analysis due to the lack of chromatographic purification.[25,29,31] Fe isotopic reference materials with high Cr contents are still lacking. Herein, four ilmenite crystals with 15-2420 μg g^{-1} Cr contents were characterized for Fe isotopic compositions by SN-MC-ICP-MS, ns-LA-MC-ICP-MS and fs-LA-MC-ICP-MS. The effectiveness of different interference correction protocols was evaluated using our ilmenites which have levels of Cr contents with 15-2420 μg g^{-1}. The analytical capability of ns-LA-MC-ICP-MS was compared to that of fs-LA-MC-ICP-MS under routine dry plasma conditions for *in situ* Fe isotopic analysis in ilmenites. Four ilmenites were evaluated as potential references for *in situ* Fe isotopic analysis.

EXPERIMENTAL

Preparation of reagents, reference materials, and ilmenite crystals. Nitric acid (HNO_3, 68%, GR grade) and hydrochloric acid (HCl, 36%, GR grade) were purified twice using a sub-boiling distillation system. Hydrofluoric acid (HF, 40%, GR grade) was purified once by a sub-boiling distillation system. Ultra-pure water with a resistivity of 18.2 MΩ×cm was obtained from a Milli-Q water purification system (Merck Millipore, Darmstadt, Germany). Ammonium bifluoride (NH_4HF_2, 98%, GR grade) was purified once using a 120 mL PFA sub-boiling bottle.

The reference materials (IRMM-014 and IRMM-524A) from the Institute for Reference Materials and Measurements (IRMM) of the European Commission were used as the external reference materials for SN-MC-ICP-MS and fs-LA-MC-ICP-MS, respectively. A stock solution of IRMM-014 (approximately 100 μg g^{-1}) was obtained from Prof. Huang Fang's group at the University of Science and Technology of China (USTC). The solution standards GSB and UIFe[5] from USTC and two geological reference materials (basalt BCR-2 and BHVO-2) were analyzed to validate the whole SN-MC-ICP-MS procedure. The Fe metal IRMM-524A

Table 1. Fe isotopic compositions of four ilmenites in different fragments obtained by SN-MC-ICP-MS

Sample		Type	$\delta^{56}Fe_{IRMM-014}$ (‰)	2sd (‰)	$\delta^{57}Fe_{IRMM-014}$ (‰)	2sd (‰)	n
RUS10	fragment-1	ilmenite	0.23	0.06	0.34	0.06	3
	fragment-2		0.23	0.06	0.36	0.13	3
	fragment-3		0.24	0.05	0.35	0.08	4
	mean		**0.24**	**0.06**	**0.35**	**0.09**	**10**
CZE2	fragment-1	ilmenite	0.15	0.07	0.28	0.13	3
	fragment-2		0.16	0.04	0.22	0.05	3
	mean		**0.16**	**0.06**	**0.25**	**0.11**	**6**
SIN1	fragment-1	ilmenite	-0.01	0.03	-0.03	0.08	3
	fragment-2		0.01	0.03	-0.01	0.05	3
	mean		**0.00**	**0.03**	**-0.02**	**0.07**	**6**
GER16	fragment-1	ilmenite	0.02	0.03	-0.02	0.08	3
	fragment-2		0.01	0.02	0.00	0.07	3
	fragment-3		-0.03	0.07	-0.04	0.11	3
	fragment-4		0.03	0.05	0.07	0.07	3
	mean		**0.01**	**0.07**	**0.00**	**0.12**	**12**
GSB	**mean**	Fe solution	**0.72**	**0.07**	**1.08**	**0.14**	**7**
	Huang et al. 2020		*0.73*	*0.05*	*1.08*	*0.10*	*39*
UIFe	**mean**	Fe solution	**0.65**	**0.04**	**1.00**	**0.08**	**7**
	Huang et al. 2020		*0.70*	*0.05*	*1.05*	*0.09*	*30*
BCR-2	**mean**	basalt	**0.07**	**0.02**	**0.14**	**0.03**	**3**
	Lei et al. 2022		*0.08*	*0.03*	*0.12*	*0.05*	*53*
BHVO-2	**mean**	basalt	**0.08**	**0.04**	**0.13**	**0.09**	**3**
	Lei et al. 2022		*0.10*	*0.03*	*0.15*	*0.06*	*56*

was used for the non-matrix-matched protocol by fs-LA-MC-ICP-MS under wet plasma conditions. Natural pyrite Aa018 was used as a quality control standard.[25]

In this study, Fe isotopic compositions of four ilmenites (RUS10, CEZ2, SIN1 and GER16) were characterized by SN-MC-ICP-MS and LA-MC-ICP-MS, respectively. Four minerals were named after locations and their approximate gram weights. It should be noted that three ilmenite crystals (RUS10, CZE2 and SIN1) have relatively homogeneous Ti isotopic compositions.[44] The photographs and typical BSE images of the four ilmenites are shown in Fig. S1. Four ilmenites showed no internal zonation or mineral inclusions, with a few fractures that need to be avoided during *in situ* analysis. The ilmenite fragments were randomly chosen from the ilmenite crystals for Fe isotopic analysis. About 2-4 fragments for each ilmenite were grinded, dissolved and measured by SN-MC-ICP-MS procedure. A few fragments of ilmenite were placed in epoxy mounts to characterize the chemical compositions and Fe isotope ratios by *in situ* laser ablation techniques.

Chemical compositions by LA-ICP-MS. Major and trace element contents of several fragments of ilmenite were measured by ICP-MS (Agilent 7900, Agilent Technology) combined with a 193 nm ns-LA system (GeoLas HD, MicroLas) at the State Key Laboratory of Geological Processes and Mineral Resources (GPMR), the China University of Geosciences (Wuhan). The National Institute of Standards and Technology (NIST) SRM 610 and the United States Geological Survey (USGS) standards (BCR-2G, BIR-1G, BHVO-2G) were used as external calibration materials. Data reduction was performed by the ICPMSDataCal program based on the sum of all metal oxides to 100 wt%.[47] The major and trace element contents of the four ilmenites are listed in Table S1.

Fe isotopic analysis by SN-MC-ICP-MS. Each ilmenite powder sample (approximately 5-10 mg) was digested with 60 mg of ammonium bifluoride (NH_4HF_2) at 230 °C for 4 h.[48] The chromatographic procedure is described in detail.[19] Briefly, 50-100 μg of Fe was purified with 0.8 mL of AG-MP-1M resin. Matrix elements (*e.g.*, Ti, Mn, Mg and Cr) were eluted with 5 mL of 8 mol L^{-1} HCl, and Fe was subsequently collected with 4 mL of 0.5 mol L^{-1} HCl and 1 mL of Milli-Q water. The Fe isotope ratio measurements were performed by a Neptune Plus MC-ICP-MS (Thermo Fisher Scientific) with a SSB method at the GPMR lab. Detailed instrumental settings are summarized in Table S2. The

IRMM-014 was adopted as the bracketing standard to correct mass bias. The concentrations of sample and bracketing standard are ≈5 μg mL^{-1}, where the ^{56}Fe signal intensity was ≈24 V. These quality control standards (GSB, UIFe, BCR-2 and BHVO-2) were analyzed to demonstrate the reliability of the procedure used for Fe isotopic analysis. Solution standard GSB and UIFe were measured by SN-MC-ICP-MS with the Fe content of 5 μg mL^{-1}. Geological reference materials (BCR-2 and BHVO-2) were measured by SN-MC-ICP-MS after dissolving and purifying. The Fe isotopic compositions obtained by SN-MC-ICP-MS are shown in Table 1.

Fe isotopic analysis by LA-MC-ICP-MS. *In situ* Fe isotopic analysis was performed by a Neptune Plus MC-ICP-MS (Thermo Fisher Scientific) combined with a 257 nm Yb:KGW fs-LA system (PHAROS, Light Conversion Ltd.) or a 193 nm ArF ns-LA system (GeoLas HD, MicroLas) at the GPMR lab. Detailed instrumental settings are summarized in Table 2. The ^{52}Cr and ^{53}Cr signal intensities were monitored to correct the isobaric interference of ^{54}Cr on ^{54}Fe. The detailed calculation is similar to that reported previously.[31] A signal smoothing device was used to improve the analytical internal precision of the Fe isotope ratio.[49] Two typical time-resolved analyses (TARs) of ilmenite GER16 obtained from fs- and ns-LA-MC-ICP-MS are shown in Fig. S2. Typical parameters of fs-LA-MC-ICP-MS were a laser spot size of 40 μm with a laser repetition rate of 3 Hz at a laser energy density of 3.2 J cm^{-2}. A laser spot size of 44 μm with a repetition rate of 3 Hz at an energy density of 4.0 J cm^{-2} was chosen for ns-LA-MC-ICP-MS. The average ^{56}Fe signal intensities of fs-LA-MC-ICP-MS and ns-LA-MC-ICP-MS were ≈22 V and ≈16 V, respectively. To carry out the wet plasma conditions, Milli-Q water was introduced online via a spray chamber equipped with a 100 μL min^{-1} PFA nebulizer.[31, 50]

One fragment of ilmenite SIN1 and Fe metal IRMM-524A as bracketing standards were used to correct instrumental drift and mass bias during *in situ* analytical sessions. Data calculation was processed using off-line Iso-Compass software.[51] All results were expressed relative to the IRMM-014 standard using δ-notation as follows:

$$\delta^{56}Fe_{\text{sample/standard}}\ (‰) = \left(\frac{(56_{Fe}/54_{Fe})_{\text{sample}} \times 2}{(56_{Fe}/54_{Fe})_{\text{standard-a}} + (56_{Fe}/54_{Fe})_{\text{standard-b}}} - 1\right) \times 1000 \quad (1)$$

$$\delta^{56}Fe_{\text{sample/IRMM-014}}\ (‰) = \delta^{56}Fe_{\text{sample/standard}} + \delta^{56}Fe_{\text{standard/IRMM-014}} \quad (2)$$

where $\delta^{56}Fe_{\text{sample/standard}}$ is the measured value of the sample relative to the bracketing standards (i.e., SIN1 and IRMM-524A) by LA-MC-ICP-MS, and $\delta^{56}Fe_{\text{standard/IRMM-014}}$ is the reference value of the bracketing standard relative to IRMM-014 determined by SN-MC-ICP-MS. The Fe isotopic compositions obtained by LA-MC-ICP-MS with different protocols are shown in Table 3.

Table 2. Operating settings of fs- and ns-LA-MC-ICP-MS

Neptune MC-ICP-MS					
Cup-configuration	L2 $^{52}Cr^+$	L1 $^{53}Cr^+$	C $^{54}(Fe + Cr)^+$	H2 $^{55}Fe^+$	H3 $^{57}Fe^+$
RF power	1200 W				
Cool gas flow	16.00 L min^{-1}				
Auxiliary gas flow	1.00 L min^{-1}				
Argon sample gas flow	0.80-1.00 L min^{-1}				
Helium carrier gas flow	0.60 L min^{-1}				
Interface cones	standard sample cone + X skimmer cone (S+X)				
Mass resolution	high resolution (Δm/m ≈8000)				
Block number	1				
Cycles of each block	120				
Integration time	0.524 s				
Laser ablation system					
Laser type	Yb:KGW femtosecond laser			ArF excimer laser	
Wavelength	257 nm			193 nm	
Pulse width	300 fs			15 ns	
Energy density	3.2 J cm^{-2}			4.0 J cm^{-2}	
Ablation mode	single spot			single spot	
Spot size	30-40 μm			32-44 μm	
Repetition rate	3-4 Hz			3-4 Hz	

RESULTS AND DISSCUSSION

Chemical and Fe isotopic compositions of the four ilmenites. Four ilmenites (RUS10, CZE2, SIN1 and GER16) were found to contain FeO from 43.6 wt% to 47.1 wt%, and TiO_2 from 44.3 wt% to 48.1 wt% (Table S1), which were homogeneous in FeO and TiO_2 contents with RSDs of <7%. However, Cr concentrations in these ilmenites varied: RUS10 with 14.9 ± 5.6 μg g^{-1} (2sd, n=32), CZE2 with 49.8 ± 28.4 μg g^{-1} (n=42), SIN1 with 1650 ± 194 μg g^{-1} (n=27) and GER16 with 2420 ± 557 μg g^{-1} (n=42). With one exception of SIN1, these ilmenites showed slightly heterogeneous Cr contents with RSDs of 12-29%. Different Cr contents (*i.e.*, different Cr/Fe ratios) in these ilmenites favor isobaric interference evaluation for *in situ* Fe isotopic analysis.

The Fe isotopic compositions of 2-4 fragments in four ilmenites and four reference materials are shown in Table 1. The GSB and UIFe standards yielded $\delta^{56}Fe_{\text{IRMM-014}}$ values of 0.72 ± 0.07‰ (2sd, n=7) and 0.65 ± 0.04‰ (2sd, n=7), respectively, whereas $\delta^{56}Fe_{\text{IRMM-014}}$ values of 0.07 ± 0.02‰ (2sd, n=3) and 0.08 ± 0.04‰ (2sd, n=3) were obtained for BCR-2 and BHVO-2, respectively. All $\delta^{56}Fe_{\text{IRMM-014}}$ results of these reference materials as quality control standards are in excellent agreement with those reported results[5,19]. Our analytical external precisions of ± 0.02-0.07‰ obtained by SN-MC-ICP-MS are comparable to those precisions of ± 0.02-0.05‰. These demonstrated the reliability of our analytical results. Finally, RUS10, CZE2, SIN1, and GER16 yielded $\delta^{56}Fe_{\text{IRMM-014}}$ values (Table 1) of 0.24 ± 0.06‰ (2sd, n=10), 0.16 ± 0.06‰ (2sd, n=6), -0.00 ± 0.03‰ (2sd, n=6) and 0.01 ± 0.07‰ (2sd, n=12), respectively. The Fe isotopic compositions in these investigated ilmenites showed a good reproducibility of ± 0.03-0.07‰, which were comparable to analytical precisions of

Table 3. Fe isotopic compositions of four ilmenites obtained by LA-MC-ICP-MS using different protocols

Sample	Analytical protocol	Bracketing standard	$\delta^{56}Fe_{IRMM-014}$ (‰)	2sd (‰)	n
RUS10	ns-LA-MC-ICP-MS + dry plasma	SIN1	0.26	0.15	42
	fs-LA-MC-ICP-MS + dry plasma	SIN1	0.23	0.14	15
	fs-LA-MC-ICP-MS + wet plasma	SIN1	0.22	0.10	59
	fs-LA-MC-ICP-MS + wet plasma	IRMM-524A	0.15	0.13	39
	SN-MC-ICP-MS	IRMM-014	0.24	0.06	10
	average value		**0.22**	**0.14**	**165**
CZE2	ns-LA-MC-ICP-MS + dry plasma	SIN1	0.14	0.16	21
	fs-LA-MC-ICP-MS + dry plasma	SIN1	0.14	0.15	35
	fs-LA-MC-ICP-MS + wet plasma	SIN1	0.15	0.12	26
	fs-LA-MC-ICP-MS + wet plasma	IRMM-524A	0.12	0.14	35
	SN-MC-ICP-MS	IRMM-014	0.16	0.06	6
	average value		**0.14**	**0.14**	**123**
SIN1	ns-LA-MC-ICP-MS + dry plasma	SIN1	0.00	0.15	15
	fs-LA-MC-ICP-MS + dry plasma	SIN1	0.01	0.14	26
	fs-LA-MC-ICP-MS + wet plasma	SIN1	0.02	0.12	28
	fs-LA-MC-ICP-MS + wet plasma	IRMM-524A	-0.04	0.13	35
	SN-MC-ICP-MS	IRMM-014	0.00	0.03	6
	average value		**0.00**	**0.14**	**110**
GER16	ns-LA-MC-ICP-MS + dry plasma	SIN1	0.02	0.16	35
	fs-LA-MC-ICP-MS + dry plasma	SIN1	-0.02	0.11	32
	fs-LA-MC-ICP-MS + wet plasma	SIN1	-0.01	0.14	46
	fs-LA-MC-ICP-MS + wet plasma	IRMM-524A	-0.02	0.14	39
	SN-MC-ICP-MS	IRMM-014	0.01	0.07	12
	average value		**0.00**	**0.14**	**164**
Aa018	fs-LA-MC-ICP-MS + wet plasma	IRMM-524A	0.52	0.10	29
	Chen et al. 2022	*Aa018*	*0.52*	*0.04*	*13*

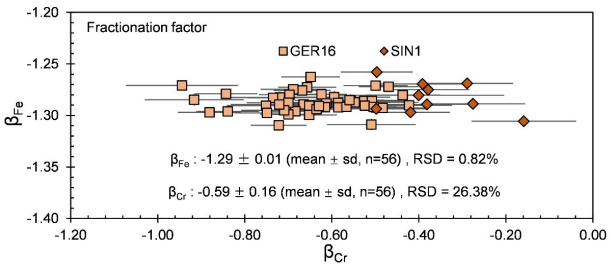

Fig. 1 Isotopic fractionation/mass bias factors (β) of Fe and Cr obtained from ilmenite SIN1 and GER16 during LA-MC-ICP-MS analysis in an analytical session. The error bars are 2SE.

our SN-MC-ICP-MS method, suggesting Fe isotopic compositions were homogeneous at the hand-specimen scale.

Evaluation of Cr interference correction protocols. The ^{54}Cr isobaric ion is the most significant interference in samples with high Cr contents for *in situ* Fe isotopic analysis.[29] The high Cr content (*e.g.*, Cr/Fe ratio > 0.0001) leads to biased Fe isotope ratios.[19,29] Our four ilmenites exhibit wide variation in Cr/Fe ratio from 0.00004 to 0.00687, consistent with the majority of natural ilmenites. The effect of ^{54}Cr on ^{54}Fe must be corrected by monitoring ^{52}Cr and/or ^{53}Cr to obtain accurate $^{56}Fe/^{54}Fe$ ratios.[29,31,52] The signal intensity of ^{52}Cr (and/or ^{53}Cr), the Cr natural isotope abundance and the instrumental mass bias factor (β) are required for *in situ* Fe isotopic analysis to subtract interferences.[29,31,52]

Herein, β_{Fe} and β_{Cr} were calculated by using a $^{57}Fe/^{56}Fe$ ratio of 0.023096 [31] and a $^{53}Cr/^{52}Cr$ ratio of 0.113386 [29] with an exponential law, respectively. The β_{Cr} and β_{Fe} were obtained from high-Cr ilmenites (SIN1 and GER16) in an analytical session (Fig. 1). As shown in Fig. 1, values for β_{Cr} showed large variation, whereas β_{Fe} values were constant. Since Cr and Fe are close in mass, mass bias should be similar for Cr and Fe.[29] The observed inaccuracy of

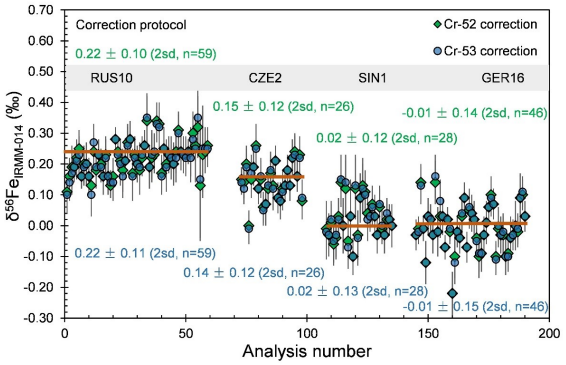

Fig. 2 Comparison of the $\delta^{56}Fe_{IRMM-014}$ values of four ilmenites obtained by LA-MC-ICP-MS using ^{52}Cr and ^{53}Cr, respectively, for isobaric interference correction in an analytical session. The error bars are 2SE. The average values from SN-MC-ICP-MS are plotted as brown lines.

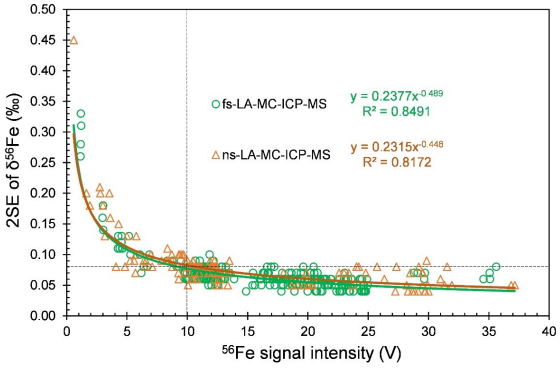

Fig. 3 Relationship between the ^{56}Fe signal intensity and individual spot precision (2SE) of $\delta^{56}Fe$ for ilmenites by ns-LA-MC-ICP-MS and fs-LA-MC-ICP-MS.

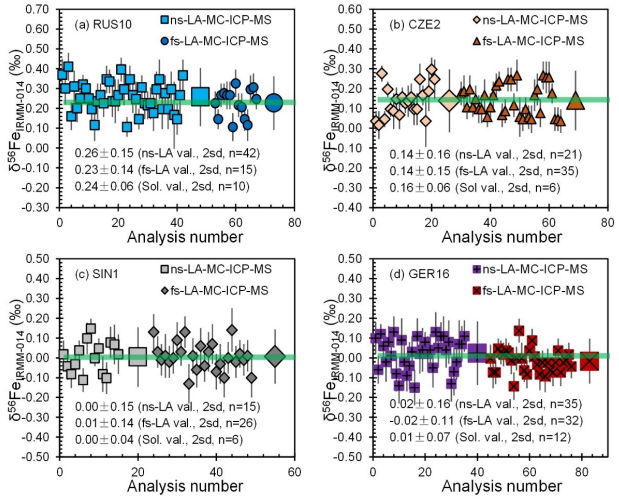

Fig. 4 Comparison of the $\delta^{56}Fe_{IRMM-014}$ values of four ilmenites obtained by ns- and fs-LA-MC-ICP-MS and by SN-MC-ICP-MS: (a) RUS10; (b) CZE2; (c) SIN1; (d) GER16. The error bars are 2SE. The average values from SN-MC-ICP-MS are plotted as green lines. Within each plot, the data are presented in chronological order. Small spot represents each analysis obtained by LA-MC-ICP-MS, while large spot represents the average value.

unstable β_{Cr} may be attributed to the low intensity of Cr during real-time analysis. β_{Fe} instead of β_{Cr} was thus chosen as the instrumental mass bias factor to correct the Cr interference. It is evident that there was no significant difference in the precision and accuracy of the $\delta^{56}Fe$ results, regardless of whether ^{52}Cr ($^{54}Cr/^{52}Cr$ ratio of 0.028226) or ^{53}Cr ($^{54}Cr/^{53}Cr$ ratio of 0.248921) was used for the correction (Fig. 2). Given the high abundance of ^{52}Cr, this isotope was chosen to correct the signal at mass 54 for the interference of ^{54}Cr on ^{54}Fe.

Analytical precisions of nanosecond and femtosecond laser systems. The internal uncertainty (*i.e.*, within-run precision or 2SE) obtained by LA-MC-ICP-MS varied from 0.05 to 0.45‰, which was greatly dependent on the Fe signal intensity but independent of the laser ablation systems (Fig. 3). As shown in Fig. 3, the ^{56}Fe signal intensity increased from 0.5 to 10 V, resulting in a significant improvement in the 2SE from 0.45 to 0.08‰. To achieve a good measurement precision of <0.08‰ (2SE), ^{56}Fe ion signals should be >10 V.

The external reproducibility (*i.e.*, external precision or 2sd) of LA-MC-ICP-MS analysis was influenced by instrument stability, mass bias correction, spectral interference correction and the homogeneity of the bracketing standard and the sample. The reproducibility of *in situ* Fe isotopic analysis was further verified by fs-LA-MC-ICP-MS and ns-LA-MC-ICP-MS under dry plasma conditions with SIN1 as the bracketing standard. Repeated analyses in several fragments of four ilmenites yielded similar external precisions (2sd) of $\delta^{56}Fe_{IRMM-014}$, i.e., ± 0.11-0.15‰ for fs-LA and ± 0.15-0.16‰ for ns-LA under dry plasma conditions (Fig. 4 and Table 3), which are comparable to those in previous reports.[22,31] Although the ns-LA system produces larger ilmenite particles than the fs-LA system,[46] the analytical precisions of the two lasers are comparable under the optimized instrumental conditions.

Results of *in situ* Fe isotopic analysis in ilmenites by LA-MC-ICP-MS. *In situ* Fe isotopic analysis in four ilmenites was conducted by ns-LA-MC-ICP-MS and fs-LA-MC-ICP-MS under dry plasma conditions using ilmenite SIN1 as the bracketing standard. The LA-MC-ICP-MS results are in agreement with the values obtained by SN-MC-ICP-MS within the analytical error (Fig. 4 and Table 3). Using a matrix-matched bracketing standard is advantageous to avoid potential matrix effect.

To further confirm the homogeneity of our ilmenites, the Fe isotopic compositions were measured by fs-LA-MC-ICP-MS under wet plasma conditions with Fe metal IRMM-524A and ilmenite SIN1 as bracketing standards, respectively. The $\delta^{56}Fe_{IRMM-014}$ value of pyrite Aa018 was 0.52 ± 0.10‰ (2sd, n=29) with Fe metal IRMM-524A as the bracketing standard, in agreement with values obtained in previous reports.[23,25] These

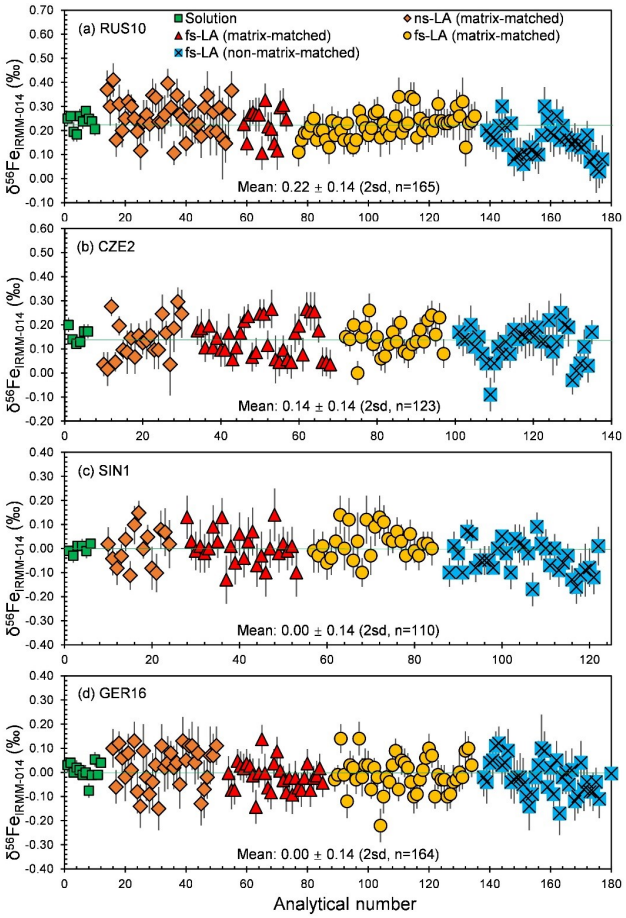

Fig. 5 Compilation of $\delta^{49}Ti_{OL\text{-}Ti}$ values of four ilmenites obtained from repeated measurements in different analytical protocols. (a) RUS10; (b) CZE2; (c) SIN1; (d) GER16. Error bars represent 2SE. The average values from SN-MC-ICP-MS are plotted as green lines. Within each plot, the data are presented in chronological order.

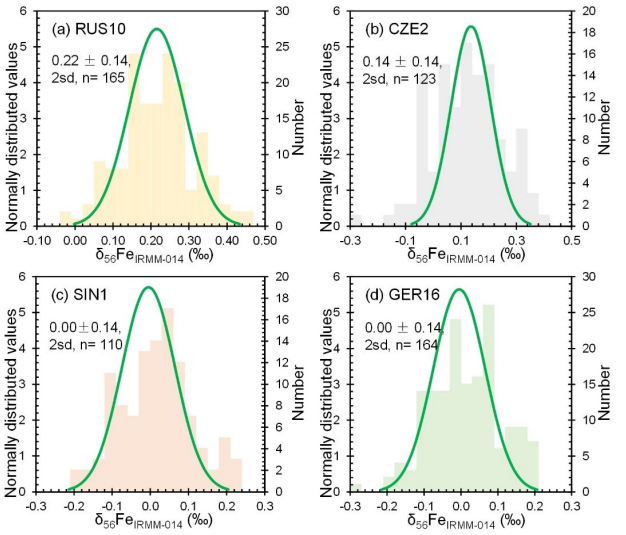

Fig. 6 Histograms of $\delta^{56}Fe_{IRMM\text{-}014}$ values of four ilmenites.

$\delta^{56}Fe_{IRMM\text{-}014}$ values of RUS10 (0.22 ± 0.10‰, 2sd, n=59), CZE2 (0.15 ± 0.12‰, n=26), SIN1 (0.02 ± 0.12‰, n=28), and GER16 (-0.01 ± 0.14‰, n=46) were obtained by fs-LA-MC-ICP-MS using SIN1 as the bracketing standard. These $\delta^{56}Fe_{IRMM\text{-}014}$ values of RUS10 (0.15± 0.13‰, n=39), CZE2 (0.12 ± 0.14‰, n=35), SIN1 (-0.04 ± 0.13‰, n=35), and GER16 (-0.02 ± 0.14‰, n=39) were obtained by fs-LA-MC-ICP-MS using IRMM-524A as the bracketing standard. Results obtained from fs-LA-MC-ICP-MS under wet plasma conditions were in agreement with values obtained by SN-MC-ICP-MS within measurement uncertainties (Fig. 5 and Table 3). It should be noted that our results from the non-matrix-matched method showed a slight systematic negative bias, *e.g.*, RUS10 ilmenite yielded 0.24 ± 0.06‰ (2sd, n=10) by SN-MC-ICP-MS and 0.15 ± 0.13‰ (2sd, n=39) by fs-LA-MC-ICP-MS with IRMM-524A as the bracketing standard. Therefore, the matrix-matched method is recommended for accurate *in situ* Fe isotopic analysis in ilmenites by LA-MC-ICP-MS.

All results for the four ilmenites from LA-MC-ICP-MS are in good agreement with the results obtained by SN-MC-ICP-MS within an analytical error of ≈ ±0.10‰ (Fig. 5 and Table 3). These ilmenites show relatively homogeneous Fe isotopic compositions, *i.e.*, 0.22 ± 0.14‰ (2sd, n=165) for RUS10, 0.14 ± 0.14‰ (2sd, n=123) for CZE2, 0.00 ± 0.14‰ (2sd, n=110) for SIN1, and 0.00 ± 0.14‰ (2sd, n=164) for GER16 (Fig. 5 and Table 3). All $\delta^{56}Fe$ results of the four ilmenites (Table S3-S7) follow Gaussian distributions (Fig. 6). Unlike ilmenites PZH12-24[31] and PZH12-18,[22] the RUS10 and CZE2 have positive δ-values, which would enrich the ilmenite reference material bank. The GER16 with high Cr content (up to 2420 μg g^{-1}) is rare in Fe isotopic microanalysis reference materials. Four tested ilmenites (RUS10, CZE2, SIN1, and GER16) are recommended as potential reference materials for LA-MC-ICP-MS analysis and can be shared with other microanalysis laboratories.

CONCLUSION

Iron isotopes in four ilmenite reference materials were determined by LA-MC-ICP-MS. The Cr interference can be effectively corrected when the Cr/Fe ratio is <0.007 using a simple protocol. The internal precision (2SE) of *in situ* Fe isotopic analysis is better than 0.08 ‰ with recorded ^{56}Fe ion signal intensity of >10 V, and the corresponding external reproducibility is ± 0.10-0.16‰ (n=15-42), which are not related to LA types. The analytical accuracy and precision of ns-LA-MC-ICP-MS are comparable to those of fs-LA-MC-ICP-MS under routine dry plasma conditions. Four tested ilmenites can serve as Fe isotopic reference materials and can be acquired from corresponding author.

ASSOCIATED CONTENT

The supporting information (Fig. S1-S2 and Table S1-S7) is available at www.at-spectrosc.com.

AUTHOR INFORMATION

Zhaochu Hu received his BSc in chemistry in 2000 from China University of Geosciences (Wuhan), and his PhD in geochemistry in 2006 from Northwest University, China. He is a research professor of analytical geochemistry at China University of Geosciences (Wuhan). His major research interests are concerned with technique and application of Laser Ablation ICP-MS/MC-ICP-MS to determine elemental and isotopic compositions of minerals, development of standard materials for microanalysis, geological sample digestion methods as well as chemical evolution and composition of the continental crust. He has been working as associate editor of *Atomic Spectroscopy* and *Roch and Mineral Analysis*, and member of editorial/advisory committee in *JAAS*, *Geostandards and Geoanalytical Research*, and *Journal of Earth Science*. Zhaochu Hu is author or co-author of over 280 articles published in peer-reviewed scientific journals, with an h-index of 51 (Web of Science). He was elected as a Fellow of the Royal Society of Chemistry in 2015 and Elsevier China Highly Cited Scholar in 2021-2022.

Corresponding Author

* Z.C. Hu

Email address: zchu@vip.sina.com

Notes

The authors declare no competing financial interest.

ACKNOWLEDGMENTS

This research is supported by the National Key R&D Program of China (2021YFC2903003), the National Natural Science Foundation of China (42330104), the Natural Science Foundation of Hubei Province (2020CFA045), and the fund from the State Key Laboratory of Geological Processes and Mineral Resources, China University of Geosciences.

REFERENCES

1. P. R. Craddock and N. Dauphas, *Geostand. Geoanal. Res.*, 2011, **35**, 101-123. https://doi.org/10.1111/j.1751-908X.2010.00085.x
2. P. P. Liu, M. F. Zhou, B. Luais, D. Cividini, and C. Rollion-Bard, *Earth Planet. Sc. Lett.*, 2014, **399**, 21-29. https://doi.org/10.1016/j.epsl.2014.05.002
3. J. Zhao, X. J. Wang, L. H. Chen, T. Hanyu, J. H. Shi, X. W. Liu, H. Kawabata, and L. W. Xie, *Contrib. Mineral. Petr.*, 2022, **177**, 101. https://doi.org/10.1007/s00410-022-01967-w
4. H. C. Tian, C. Zhang, F. Z. Teng, Y. J. Long, S. G. Li, Y. S. He, S. Ke, X. Y. Chen, and W. Yang, *Geochim. Cosmochim. Ac.*, 2020, **278**, 361-375. https://doi.org/10.1016/j.gca.2019.10.004
5. J. Huang, S. Guo, Q. Z. Jin, and F. Huang, *Geochim. Cosmochim. Ac.*, 2020, **278**, 376-391. https://doi.org/10.1016/j.gca.2019.06.020
6. S. Graham, N. Pearson, S. Jackson, W. Griffin, and S. Y. O'Reilly, *Chem. Geol.*, 2004, **207**, 147-169. https://doi.org/10.1016/j.chemgeo.2004.02.009
7. I. Horn, F. v. Blanckenburg, R. Schoenberg, G. Steinhoefel, and G. Mark, *Geochim. Cosmochim. Ac.*, 2006, **70**, 3677-3688. https://doi.org/10.1016/j.gca.2006.05.002
8. R. A. Wiesli, B. L. Beard, L. A. Taylor, and C. M. Johnson, *Earth Planet. Sc. Lett.*, 2003, **216**, 457-465. https://doi.org/10.1016/s0012-821x(03)00552-1
9. S. Weyer, A. Anbar, G. Brey, C. Munker, K. Mezger, and A. Woodland, *Earth Planet. Sc. Lett.*, 2005, **240**, 251-264. https://doi.org/10.1016/j.epsl.2005.09.023
10. S. M. Elardo and A. Shahar, *Nat. Geosci.*, 2017, **10**, 317-321. https://doi.org/10.1038/ngeo2896
11. Y. Jiang, J. T. Kang, S. Y. Liao, S. M. Elardo, K. Q. Zong, S. J. Wang, C. Nie, P. Y. Li, Z. J. Yin, F. Huang, and W. B. Hsu, *Astrophys. J. Lett.*, 2023, **945**, L26. https://doi.org/10.3847/2041-8213/acbd31
12. Y. B. Cheng, J. W. Mao, X. K. Zhu, and Y. Wang, *Gondwana Res.*, 2015, **27**, 1283-1291. https://doi.org/10.1016/j.gr.2013.12.006
13. H. Q. Wei, H. C. Tian, S. G. Li, W. Yang, B. Y. Gao, S. Ke, R. Y. Li, X. W. Chen, and H. M. Yu, *Chem. Geol.*, 2021, **565**, 120075. https://doi.org/10.1016/j.chemgeo.2021.120075
14. N. Dauphas, S. G. John, and O. Rouxel, *Rev. Mineral. Geochem.*, 2017, **82**, 415-510. https://doi.org/10.2138/rmg.2017.82.11
15. N. X. Nie, N. Dauphas, E. E. Alp, H. Zeng, C. K. Sio, J. Y. Hu, X. Chen, S. M. Aarons, Z. Zhang, H. C. Tian, D. Wang, K. B. Prissel, J. Greer, W. Bi, M. Y. Hu, J. Zhao, A. Shahar, M. Roskosz, F. Teng, M. J. Krawczynski, P. R. Heck, and F. S. Spear, *Geochim. Cosmochim. Ac.*, 2021, **302**, 18-45. https://doi.org/10.1016/j.gca.2021.03.014
16. D. M. Borrok, R. B. Wanty, W. I. Ridley, R. Wolf, P. J. Lamothe, and M. Adams, *Chem. Geol.*, 2007, **242**, 400-414. https://doi.org/10.1016/j.chemgeo.2007.04.004
17. N. Dauphas, A. Pourmand, and F. Z. Teng, *Chem. Geol.*, 2009, **267**, 175-184. https://doi.org/10.1016/j.chemgeo.2008.12.011
18. J. Wang, D. M. Tang, B. X. Su, Q. H. Yuan, W. J. Li, B. Y. Gao, K. Y. Chen, Z. A. Bao, and Y. Zhao, *J. Anal. At. Spectrom.*, 2022, **37**, 1869-1875. https://doi.org/10.1039/d2ja00084a
19. Y. T. Lei, M. Li, Z. C. Wang, Y. T. Zhu, Z. C. Hu, Y. S. Liu, and X. N. Chai, *Atom. Spectrosc.*, 2022, **43**, 214-222. https://doi.org/10.46770/AS.2022
20. W. Zhang and Z. C. Hu, *Spectrochim. Acta B*, 2020, **171**, 105929. https://doi.org/10.1016/j.sab.2020.105929
21. T. Hirata, Y. Hayano, and T. Ohno, *J. Anal. At. Spectrom.*, 2003, **18**, 1283-1288. https://doi.org/10.1039/b305127g

22. L. Xu, J. H. Yang, H. Wang, L. W. Xie, Y. H. Yang, C. Huang, and S. T. Wu, *J. Anal. At. Spectrom.*, 2022, **37**, 1835-1845. https://doi.org/10.1039/d2ja00151a
23. Y. T. Feng, W. Zhang, Z. C. Hu, T. Luo, M. Li, Y. S. Liu, H. Liu, and Q. L. Li, *J. Anal. At. Spectrom.*, 2022, **37**, 551-562. https://doi.org/10.1039/d1ja00392e
24. X. Y. Zheng, B. L. Beard, and C. M. Johnson, *J. Anal. At. Spectrom.*, 2018, **33**, 68-83. https://doi.org/10.1039/c7ja00272f
25. K. Y. Chen, H. L. Yuan, Z. A. Bao, and N. Lv, *Atom. Spectrosc.*, 2021, **42**, 282-293. https://doi.org/10.46770/as.2021.703
26. L. Chen, Y. Liu, Y. Li, Q. L. Li, and X. H. Li, *J. Anal. At. Spectrom.*, 2021, **36**, 1431-1440. https://doi.org/10.1039/d1ja00029b
27. Y. T. Feng, W. Zhang, Z. C. Hu, T. Luo, Q. L. Li, and J. Y. Li, *Geostand. Geoanal. Res.*, 2023. https://doi.org//10.1111/ggr.12530
28. C. G. d. Vega, M. Costas-Rodriguez, T. V. Acker, S. Goderis, and F. Vanhaecke, *Anal. Chem.*, 2020, **92**, 3572-3580. https://doi.org/10.1021/acs.analchem.9b04029
29. L. Xu, W. Zhang, T. Luo, J. H. Yang, and Z. C. Hu, *J. Anal. At. Spectrom.*, 2021, **36**, 747-757. https://doi.org/10.1039/d0ja00465k
30. Q. C. Yang, H. M. Gong, X. H. Wang, M. Duan, Y. Y. Xiao, and W. D. Sun, *J. Anal. At. Spectrom.*, 2022, **37**, 1000-1009. https://doi.org/10.1039/d1ja00410g
31. L. Xu, J. H. Yang, L. W. Xie, H. Wang, Y. H. Yang, C. Huang, and S. T. Wu, *Spectrochim. Acta B*, 2022, **189**, 106374. https://doi.org/10.1016/j.sab.2022.106374
32. W. Dziony, I. Horn, D. Lattard, J. Koepke, G. Steinhoefel, J. A. Schuessler, and F. Holtz, *Chem. Geol.*, 2014, **363**, 101-113. https://doi.org/10.1016/j.chemgeo.2013.10.035
33. L. Chen, Y. T. Feng, H. M. Yu, W. Zhang, J. T. Kang, F. Huang, Z. C. Hu, and X. H. Li, *J. Anal. At. Spectrom.*, 2022, **37**, 2300-2308. https://doi.org/10.1039/d2ja00002d
34. E. S. Steenstra, J. Berndt, S. Klemme, W. v. Westrenen, E. S. Bullock, and A. Shahar, *J. Anal. At. Spectrom.*, 2020, **35**, 498-509. https://doi.org/10.1039/c9ja00391f
35. Q. L. Li, Q. Zhou, Y. Liu, Z. Y. Xiao, Y. T. Lin, J. H. Li, H. X. Ma, G. Q. Tang, S. Guo, X. Tang, J. Y. Yuan, J. Li, F. Y. Wu, Z. Y. Ouyang, C. L. Li, and X. H. Li, *Nature*, 2021, **600**, 54-58. https://doi.org/10.1038/s41586-021-04100-2
36. J. M. Thompson, K. Goemann, I. Belouson, K. Jenkin, A. Kobussen, W. Powell, and L. Danyushevsky, *J. Anal. At. Spectrom.*, 2021, **36**, 1244-1260. https://doi.org/10.1039/d1ja00069a
37. Y. Q. Wei, Y. L. Niu, H. M. Gong, M. Duan, S. Chen, P. Y. Guo, and P. Sun, *Gondwana Res.*, 2020, **81**, 240-251. https://doi.org/10.1016/j.gr.2019.12.001
38. A. Rahman, J. Tardio, S. K. Bhargava, M. N. Zaman, A. S. M. M. Hasan, A. Torpy, and M. I. Pownceby, *Ore Geol. Rev.*, 2020, **117**, 103271. https://doi.org/10.1016/j.oregeorev.2019.103271
39. Y. Zhao, J. d. Vries, A. P. v. d. Berg, M. H. G. Jacobs, and W. v. Westrenen, *Earth Planet. Sc. Lett.*, 2019, **511**, 1-11. https://doi.org/10.1016/j.epsl.2019.01.022
40. J. d. Vries, A. v. d. Berg, and W. v. Westrenen, *Earth Planet. Sc. Lett.*, 2010, **292**, 139-147. https://doi.org/10.1016/j.epsl.2010.01.029
41. P. H. Donohue, A. Simonetti, and C. R. Neal, *Geostand. Geoanal. Res.*, 2012, **36**, 61-73. https://doi.org/10.1111/j.1751-908X.2011.00124.x
42. C. E. Morisset, J. S. Scoates, D. Weis, and A. Rahier, *Geostand. Geoanal. Res.*, 2014, **38**, 159-176. https://doi.org/10.1111/j.1751-908X.2013.00207.x
43. C. Huang, H. Wang, L. W. Xie, N. X. Nie, Y. H. Yang, X. M. Zhao, J. Li, H. C. Tian, S. T. Wu, L. Xu, and J. H. Yang, *J. Anal. At. Spectrom.*, 2022, **37**, 2165-2175. https://doi.org/10.1039/d2ja00189f
44. H. Liu, Z. B. Deng, Z. C. Hu, W. Zhang, M. Schiller, M. Bizzarro, Y. S. Liu, Z. C. Wang, L. P. Feng, and M. Li, *Geostand. Geoanal. Res.*, 2023, online published. https://doi.org/10.1111/ggr.12525
45. K. Y. Chen, Z. A. Bao, H. L. Yuan, and N. Lv, *J. Anal. At. Spectrom.*, 2022, **37**, 249-263. https://doi.org/10.1039/d1ja00381j
46. Z. Li, Z. C. Hu, D. Günther, K. Q. Zong, Y. S. Liu, T. Luo, W. Zhang, S. Gao, and S. H. Hu, *Geostand. Geoanal. Res.*, 2016, **40**, 477-491. https://doi.org/10.1111/ggr.12117
47. Y. S. Liu, Z. C. Hu, S. Gao, D. Günther, J. Xu, C. G. Gao, and H. H. Cheng, *Chem. Geol.*, 2008, **257**, 34-43. https://doi.org/10.1016/j.chemgeo.2008.08.004
48. H. Liu, Z. C. Hu, T. He, W. Zhang, K. Q. Zong, T. Luo, X. Y. Qiu, Y. Gao, and M. F. Li, *J. Anal. At. Spectrom.*, 2023, **38**, 1146-1154. https://doi.org/10.1039/d3ja00012e
49. Z. C. Hu, Y. S. Liu, S. Gao, S. Q. Xiao, L. S. Zhao, D. Günther, M. Li, W. Zhang, and K. Q. Zong, *Spectrochim. Acta B*, 2012, **78**. 50-57. https://doi.org/10.1016/j.sab.2012.09.007
50. H. Liu, W. Zhang, Z. B. Deng, Z. C. Hu, M. Schiller, M. Bizzarro, Y. S. Liu, T. Luo, Y. T. Feng, and L. P. Feng, *Spectrochim. Acta B*, 2023, **202**, 106646. https://doi.org/10.1016/j.sab.2023.106646
51. W. Zhang, Z. C. Hu, and Y. S. Liu, *J. Anal. At. Spectrom.*, 2020, **35**, 1087-1096. https://doi.org/10.1039/d0ja00084a
52. J. Košler, R. B. Pedersen, C. Kruber, and P. J. Sylvester, *J. Anal. At. Spectrom.*, 2005, **20**, 192-199. 10.1039/b412169d